Journal of Bio- and Tribo-Corrosion (2019) 5:4
https://doi.org/10.1007/s40735-018-0195-3

# Electrochemical Studies on New Pyridazinium Derivatives as Corrosion Inhibitors of Carbon Steel in Acidic Medium

F. El Hajjaji[1] · R. Salim[1,2] · M. Messali[3] · B. Hammouti[4] · D. S. Chauhan[5] · S. M. Almutairi[6] · M. A. Quraishi[5]

Received: 3 July 2018 / Revised: 3 October 2018 / Accepted: 20 October 2018 / Published online: 2 November 2018


**Abstract**
Two pyridazine derivatives "1-decylpyridazin-1-ium iodide" (DPI) and "1-tetradecylpyridazin-1-ium iodide" (TPI) were synthesized and investigated as corrosion inhibitors for carbon steel in HCl (1 M) solution. In order to evaluate the anticorrosion activity of these compounds, the electrochemical impedance spectroscopy was performed at different concentrations and at various temperatures (303–333 K). The collected results showed that DPI and TPI reached a value of 86.7% and 88.6% at $10^{-3}$ M, respectively (303 K). The decrease of the double-layer capacitance for TPI became more remarkable with increase in temperature. The adsorption of both inhibitors on mild steel surface obeyed the Langmuir adsorption isotherm. An inhibition efficiency of 97.6% was obtained at the optimum concentration ($10^{-3}$ M) following an immersion period of 12 h. The quantum chemical calculations based on DFT method supported the experimentally obtained results.

**Keywords** Pyridazinium · Ionic liquids · Impedance · Langmuir isotherm · Adsorption · Immersion time

## 1 Introduction

The carbon steel is commonly used in a number of industries due to its low cost and good mechanical properties [1–4]. On the other hand, the acidic medium especially hydrochloric acid is widely used in industrial processes such as acid cleaning, acid descaling, and acid pickling. In order to reduce the corrosive attack of acid on steel surface, certain chemical compounds are added to the acid solution. This practice of introducing the corrosion inhibitors to the aggressive acidic medium is one of the most commonly used methods to counter the corrosion of carbon steel. Organic corrosion inhibitors act by adsorption, which is facilitated by the presence of heteroatoms such as nitrogen, oxygen, sulfur, presence of double bonds, and aromatic rings [5–11]. Many *N*-heterocyclic compounds such as the derivatives of imidazole [12, 13], pyrazole [14], pyrimidine [15], and imidazolopyridine [16, 17] have been reported as effective corrosion inhibitors for carbon steel in acidic solution.

The use of ionic liquids for a wide range of applications is gaining significance particularly in the field of fundamental chemistry and chemical engineering [18]. Currently, ionic liquids have application in many fields such as solvents or catalysts for chemical synthesis [19], media for electrodeposition of metals [20], supercapacitors [21], electrolyte for electrochemical devices such as battery [22] and corrosion inhibitors [23, 24]. The use of this type of molecules leads to a large reduction in reaction times with several advantages of the eco-friendly approach and is therefore considered as green technology [25, 26]. The fascinating properties of ionic liquids such as high polarity, low melting points, low vapor pressure, low toxicity, high thermal and chemical stability, less hazardous influence on environment and living beings make them as a promising candidate for replacing

✉ M. A. Quraishi
maquraishi.apc@itbhu.ac.in

1 Laboratory of Engineering, Electrochemistry, Modeling and Environment, Faculty of Sciences, University sidi Mohamed Ben Abdellah, 30000 Fez, Morocco

2 Laboratory of Separation Processes, Faculty of Science, University Ibn Tofail, Kenitra, Morocco

3 Chemistry Department, Faculty of Sciences, Taibah University, Al-Madinah Al-Mounawara 30002, Saudi Arabia

4 LCAE-URAC 18, Faculty of Science, First Mohammed University, PO Box 717, 60000 Oujda, Morocco

5 Center of Research Excellence in Corrosion, Research Institute, King Fahd University of Petroleum and Minerals, Dhahran 31261, Saudi Arabia

6 King Abdulaziz City for Science and Technology, P.O. Box 6086, Riyadh 11442, Saudi Arabia

the conventionally used highly volatile and toxic corrosion inhibitors [18].

In the light of above, in the present work, two newly synthesized pyridazine derivatives "1-decylpyridazin-1-ium iodide" (DPI) and "1-tetradecylpyridazin-1-ium iodide" (TPI) were examined as corrosion inhibitors of carbon steel in 1.0 M HCl. These compounds have not been reported previously as corrosion inhibitors. In addition, the synthesis procedure only requires a single-step reaction. Furthermore, the derivatives afford excellent solubility in hydrochloric acid solution and the presence of pyridazine ring along with the hydrocarbon tail is expected to facilitate their adsorption and corrosion inhibition behavior. We have chosen the ionic liquids having different carbon chain lengths to see their comparative influence on the inhibition performance. The inhibition activity of these organic compounds was evaluated by electrochemical impedance spectroscopy (EIS). The different thermodynamic and kinetic adsorption parameters for corrosion inhibition process are evaluated. Furthermore, the adsorption of pyridazinium derivatives on the metal/electrolyte interface of the metal was studied at longer immersion times in order to understand the interactions between pyridazinium derivatives and steel surface. Quantum chemical calculations using the Density functional theory (DFT) method was also used to study the mechanism of steel corrosion inhibition of the synthesized ionic liquids in acidic medium.

## 2 Experimental

### 2.1 Specimens and Solution Preparation

The steel sample used in this study is a carbon steel (CS) having chemical composition (in wt%) of 99.21% Fe, 0.38% Si, 0.21% C, 0.05% Mn, 0.05% S, 0.09% P, and 0.01% Al. The aggressive solution of 1.0 M HCl was prepared by dilution of analytical grade 37% HCl with distilled water. The concentration range of the studied compounds was $10^{-6}$–$10^{-3}$ M.

### 2.2 General Procedure for Synthesis of Inhibitors DPI and TPI

DPI: Pyridazine (1eq) and 1-iododecane (1eq) were placed in a Pyrex glass beaker and exposed to irradiation for 5 h at room temperature using an ultrasonic bath. Completion of the reaction was marked by the precipitation of a solid from the initially obtained clear and homogenous mixture in toluene. The pyridazinium salt was isolated by filtration and washed three times with ethyl acetate to remove any unreacted starting materials and solvent. Finally, the salt DPI was dried at reduced pressure to remove all volatile organic compounds (Figs. 1, 2).

DPI: Yellow crystals, MP 83–84 °C, 1H NMR (DMSO, 400 MHz,): δ = 0.85 (t, 3H, $CH_3$), 1.24–1.30 (m, 14H, $CH_2$), 1.99 (quint, 2H, $CH_2$), 4.82 (t, 2H, $NCH_2$), 8.63 (t, 1H, CH), 8.76 (t, 1H, CH), 9.65 (d, 1H, CH), 9.97 (d, $^1$H, CH); $^{13}$C NMR (DMSO, 100 MHz,): δ = 14.4 ($CH_3$), 22.7 ($CH_2$), 28.8 ($CH_2$), 29.2 ($CH_2$), 29.3 ($CH_2$), 29.4 ($CH_2$), 29.5 ($CH_2$), 29.9 ($CH_2$), 31.7 ($CH_2$), 65.0 ($CH_2$), 136.5 (CH), 137.0 (CH), 150.3 (CH), 154.9 (CH); IR (νmax $cm^{-1}$) 3129 (C–H, sp2), 1559–1469 (C=C), 1163 (C–N), 1080 (C–O); LCMS (M–I) 221.2 found for $C_{14}H_{25}N_2^+$.

TPI: Pyridazine (1eq) and 1-iodotetradecane (1eq) were placed in a glass beaker and exposed to ultrasonic irradiation for 5 h at room temperature as mentioned above for DPI. Completion of the reaction was marked by the precipitation of a solid from the initially obtained clear and homogenous mixture in toluene. The pyridazinium salt was isolated by filtration and washed three times with ethyl acetate to remove any unreacted starting materials and solvent. Finally, the salt TPI was dried at a reduced pressure to remove all volatile organic compounds (Figs. 3, 4).

TPI: white crystals, MP 117–119 °C, $^1$H NMR (DMSO, 400 MHz,): δ = 0.84 (t, 3H, $CH_3$), 1.21–1.33 (m, 18H, $CH_2$), 1.37 (m, 4H, $CH_2$), 2.10 (quint, 2H, $CH_2$), 5.05 (t, 2H, $CH_2$), 8.80 (t, 1H, CH), 9.00 (t, 1H, CH), 9.52 (d, 1H, CH), 10.95 (d, 1H, CH); $^{13}$C NMR (DMSO, 100 MHz,): δ = 19.2 ($CH_3$), 27.3 ($CH_2$), 30.6 ($CH_2$), 33.6 ($CH_2$), 33.8 ($CH_2$), 33.9 ($CH_2$), 34.6 ($CH_2$), 36.4 ($CH_2$), 69.8 ($CH_2$), 141.2 (CH), 141.8 (CH), 155.1 (CH), 159.8 (CH); IR (νmax $cm^{-1}$) 3132 (C–H, sp2), 1561–1472 (C=C), 1165 (C–N), 1083(C–O); LCMS (M–I) 277.2 found for $C_{18}H_{33}N_2^+$. Scheme 1 represent the structures of ionic liquids (DPI) and (TPI).

### 2.3 Electrochemical Measurements

Electrochemical experiments were performed using a Radiometer analytical (VoltaLab-PGZ 100), coupled to a computer equipped with a software Voltamaster 4. The experiments were performed in a three-electrode cell where the working electrode was a carbon steel with a surface area of 1 $cm^2$. Before each experiment, the electrode was polished with emery paper until 1500 grade and cleaned with distilled water. The counter electrode used was a platinum plate and a saturated calomel electrode (SCE) was used as the reference electrode. The measurements of electrochemical impedance spectroscopy (EIS) were performed using AC signals of amplitude 10 mV peak to peak at different conditions in the frequency range of 100 kHz–10 mHz.

The charge transfer resistance $R_{ct}$ was obtained from the diameter of the semicircle in the Nyquist representation. Thus, the inhibition efficiency was calculated using the following equation:

$$E\% = \frac{R_{ct} - R_{ct(inh)}}{R_{ct}} \times 100,$$

where $R_{ct}$ and $R_{ct(inh)}$ are the charge transfer resistances in the absence and in presence of inhibitor, respectively.

## 2.4 Quantum Study

Quantum chemical computations were carried out by density function theory (DFT) using 6-31G (d, p) basis set for all atoms. All the calculations were carried out with Gaussian 09W package. The following quantum chemical parameters were acquired: $E_{HOMO}$, $E_{LUMO}$, the energy gap (ΔE), electronegativity ($\chi$), global hardness ($\eta$), global softness ($\sigma$), fraction of electrons transferred (ΔN), and the dipole moment ($\mu$).

The absolute electronegativity ($\chi$) is a measure of the power of an atom or a group of atoms to attract electrons to itself and can be approximated as follows:

$$\chi = \frac{1}{2}(E_{HOMO} + E_{LUMO}).$$

The hardness ($\eta$) and softness ($\sigma$) are global chemical descriptors measuring the molecular stability and reactivity and are given in the following equations:

$$\eta = \frac{1}{2}(E_{HOMO} - E_{LUMO});\ \sigma = 1/\eta.$$

The dipole moment ($\mu$) is another index that is often used for the prediction of a corrosion inhibition process. It is a measure of polarity in a certain bond and it is related to the distribution of electrons in a certain molecule [27]. The fraction of electrons transferred from the molecule to the surface of metal (ΔN) was estimated according to Pearson theory [28] by using the following equation:

$$\Delta N = \frac{\chi_{Fe} - \chi_{inh}}{2(\eta_{Fe} + \eta_{inh})},$$

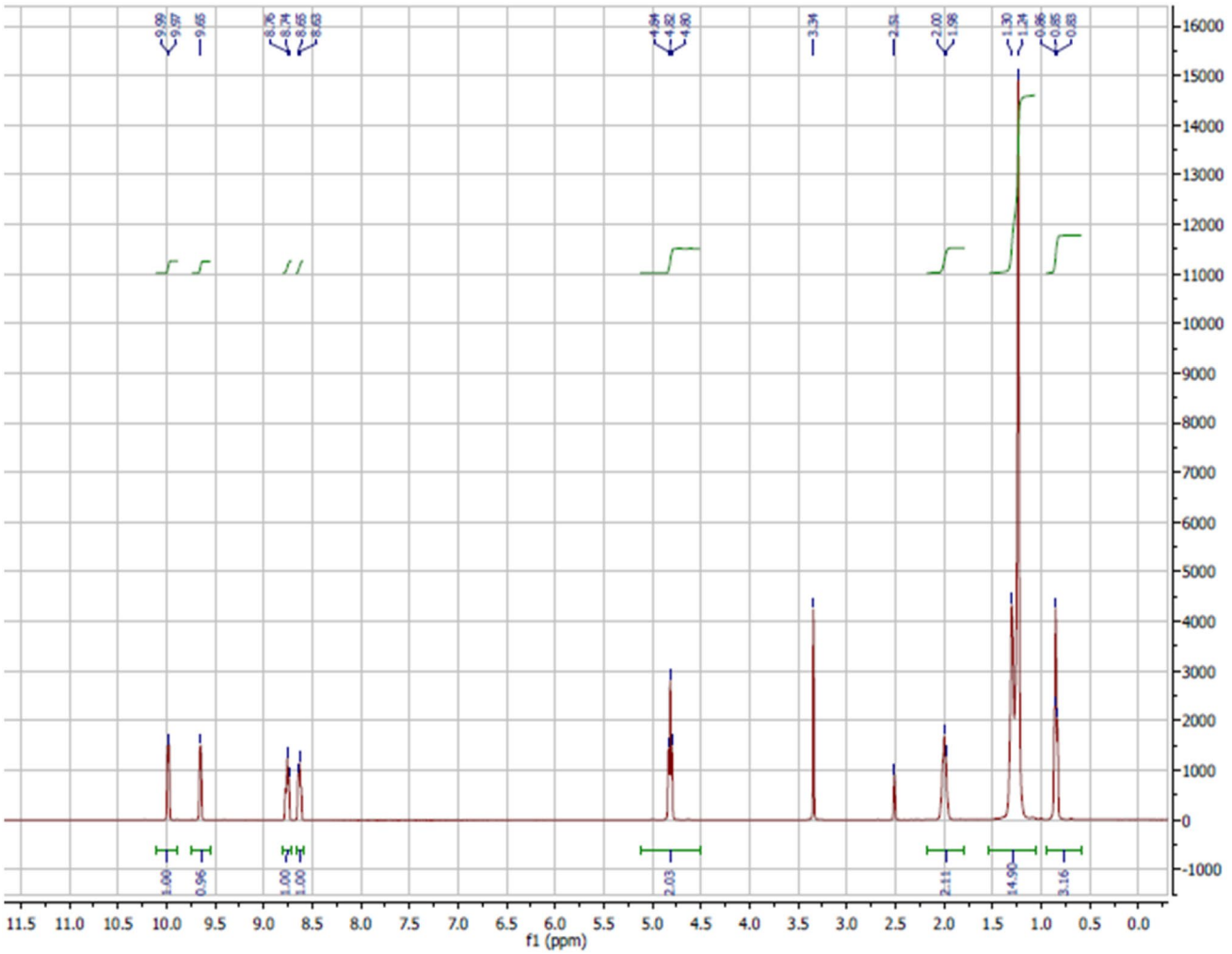


**Fig. 1** $^1$H NMR spectrum of 1-decylpyridazin-1-ium iodide (DPI)

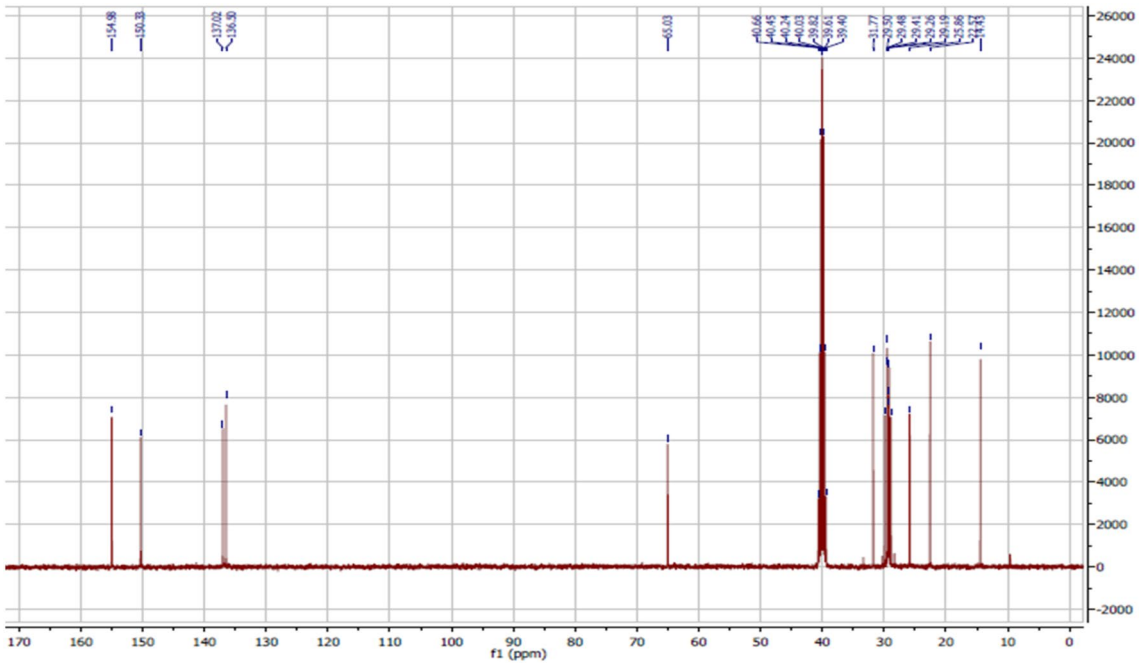


**Fig. 2** $^{13}$C NMR spectrum of 1-decylpyridazin-1-ium iodide (DPI)

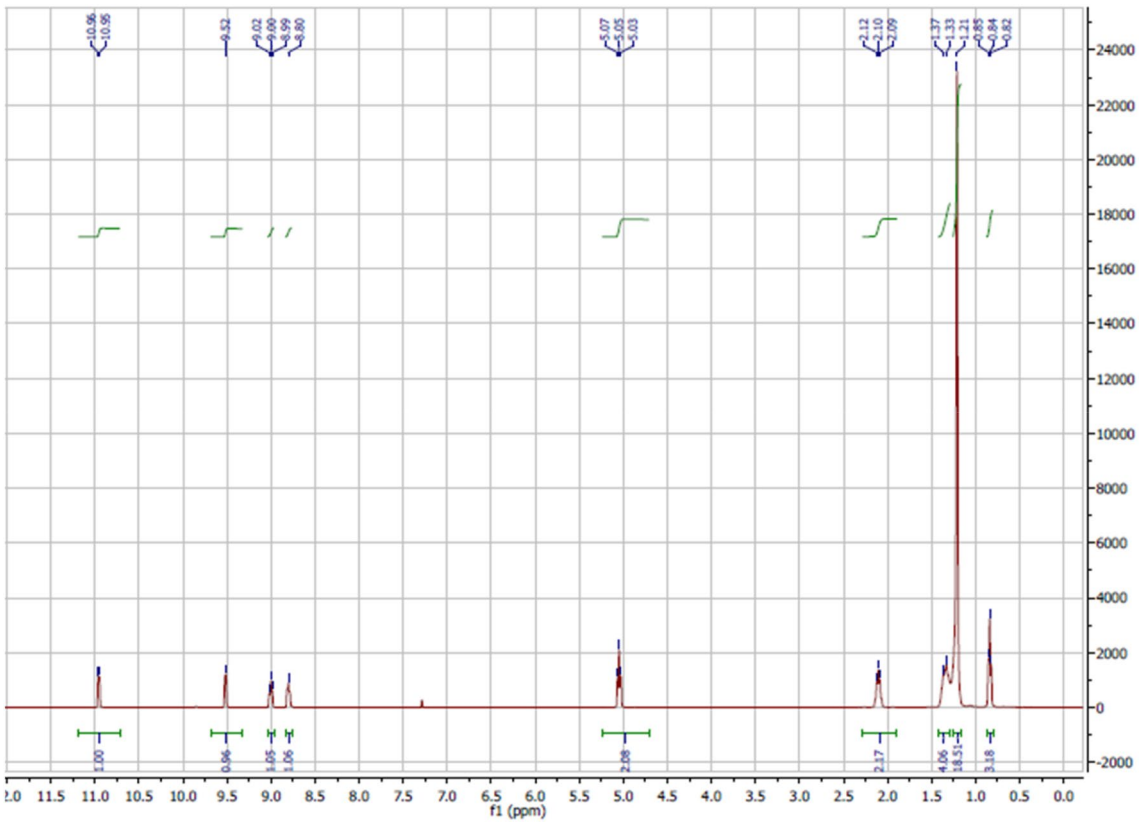


**Fig. 3** $^{1}$H NMR spectrum of 1-tetradecylpyridazin-1-ium iodide (TPI)

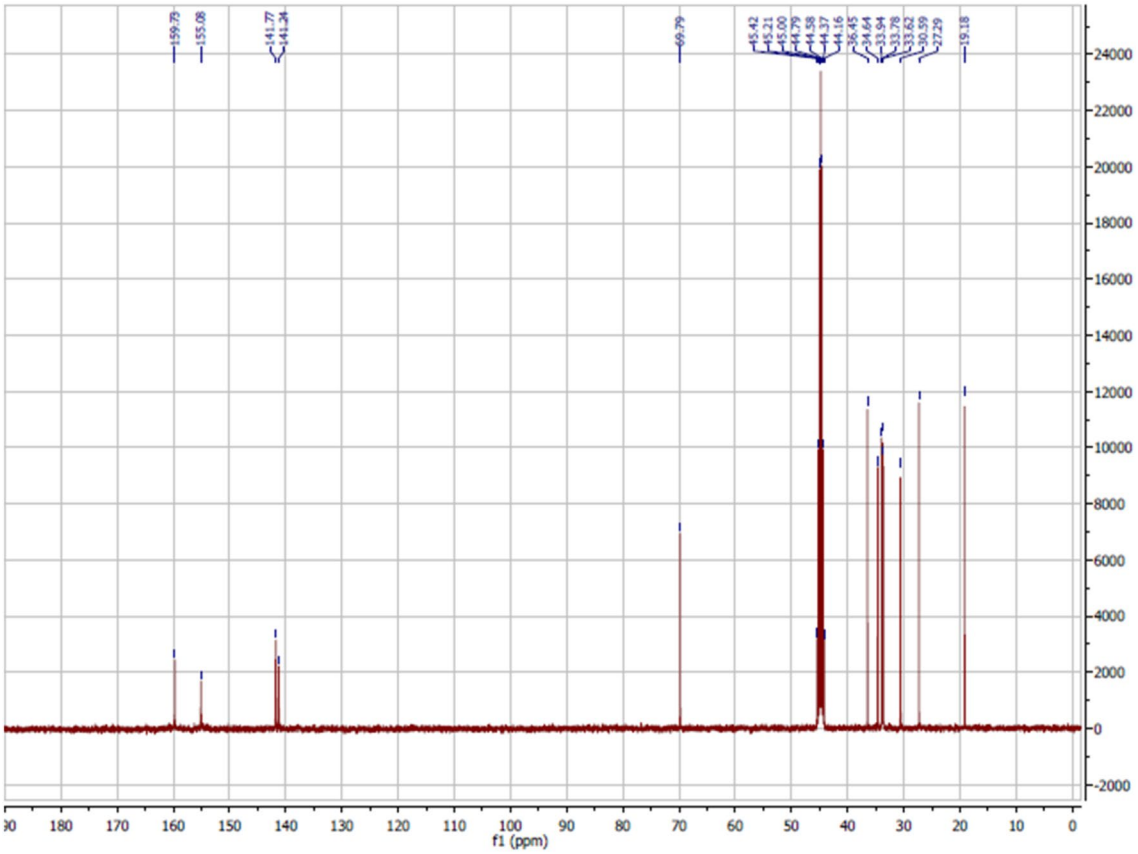


**Fig. 4** $^{13}$C NMR spectrum of 41-tetradecylpyridazin-1-ium iodide (TPI)

where a theoretical value for the electronegativity of bulk iron was used, $\chi_{Fe} = 7$ eV, and a global hardness of $\eta_{Fe} = 0$ was used.

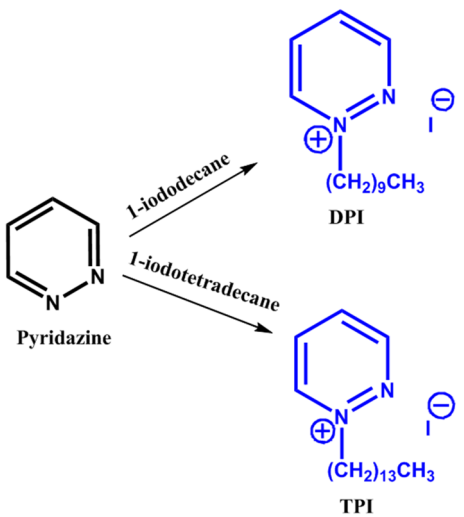


**Scheme 1** Schematic representation of the structures of ionic liquids (DPI) and (TPI)

## 3 Results and Discussion

### 3.1 Effect of Inhibitor Concentration

Figure 5 illustrates the representative Nyquist plots of carbon steel in 1.0 M HCl solution in the absence and presence of various concentrations of DPI and TPI after immersion for 30 min at 303 K.

As shown in Fig. 5, it can be observed that the diameter of the capacitive loop in the presence of the inhibitors is greater than in the uninhibited solution and increases with increase in the concentration of inhibitors. It is obvious that these capacitive loops are not perfect semicircles which can be attributed to the frequency dispersion effect as a result of the roughness and inhomogeneity of the steel surface [29–31].

The equivalent circuit models used to fit the experimentally obtained Nyquist data are shown in Fig. 6. Generally the frequency dispersion is frequently modeled by using constant phase element ($Q$), the circuit used for compound DPI (a) has a CPE constant $Q_r$ which is in parallel with charge transfer resistance $R_{ct}$ and together they are in series with the solution resistance $R_s$. The circuit obtained for TPI (b) has

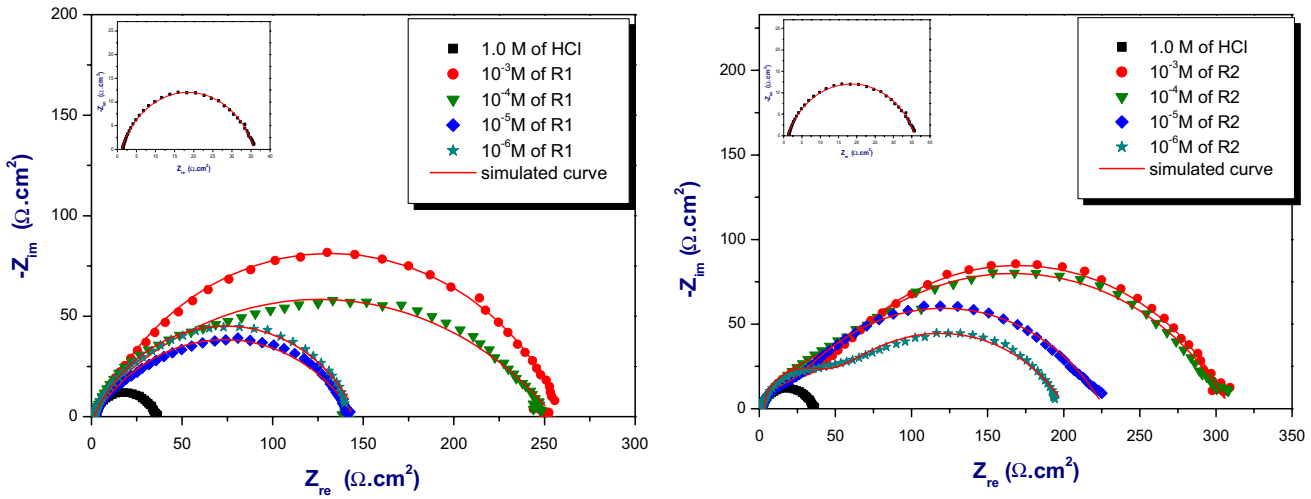


**Fig. 5** Nyquist plots and simulation curves of carbon steel in 1.0 M HCl with different concentrations of DPI (R1) and TPI (R2) at 303 K

an additional resistance component ($R_f$) and a second CPE ($Q_{dl}$) which are not observed for circuit (a).

The equation which relates the double-layer capacitance ($C_{dl}$) to the transfer charge resistance $R_{ct}$ and the CPE constant (Q) is described as follows [32]:

$$C_{dl} = \left(Q \times {R_{ct}}^{1-n}\right)^{1/n},$$

where $Q$ is the proportional factor and n is the CPE exponent which is related to the surface inhomogeneity. The electrochemical parameters such as charge transfer resistance $R_{ct}$, double-layer capacitance $C_{dl}$, and corrosion inhibition efficiency (IE) are given in Table 1.

It can be observed from the impedance data (Table 1) that the value of $R_{ct}$ increases with increase in the concentration of inhibitors which also indicates an increase in the corrosion inhibition efficiency which attains a maximum value of 86.7% for DPI and 88.6% for TPI at a concentration of $10^{-3}$ M. It can also be observed that the double-layer capacitance $C_{dl}$ decreased with increase in the inhibition efficiency which can be explained with the adsorption of the inhibitor onto the carbon steel surface after the displacement of water molecules and other ions which are already adsorbed onto the steel surface. The decrease in the double-layer capacitance $C_{dl}$ can be explained using Helmholtz model [33]:

$$C_{dl} = \frac{\varepsilon\varepsilon_0}{d}S,$$

where $\varepsilon$ is the dielectric constant of the medium, $\varepsilon_0$ is the permittivity of the free space, S is the effective surface area of the working electrode, and d is the thickness of the electrical double layer formed by the adsorbed inhibitors. Considering the second inhibitor (TPI), the data also illustrate an increase in the diameter of the capacitive loop. These results suggest that a protective film of inhibitor molecules was formed on the electrode surface [34, 35].

As an example, the fitted Bode diagrams for inhibited solution at the optimum concentration are presented in Fig. 7 (DPI) and Fig. 8 (TPI).

From the results it can be observed that the Bode and phase angle plots for DPI show a one-time constant process while those for TPI show a two-time constant process [36, 37] The relaxation time of a surface state is the time required for the return of the charge distribution to the equilibrium point after an electrical disturbance, it can be defined as [38]

$$\tau = C_{dl}R_{ct}.$$

The adsorption of an inhibitor molecule requires some time to attain equilibrium. If this time is very small, only the time constant for double-layer charging would be expressed as observed in case of DPI. The appearance of a second time constant in case of TPI can be attributed to the requirement of more time by the system to reach the adsorption equilibrium. In this case, a process having an additional time constant is added to the double-layer charging process. It is obvious that in such case the description cannot be made using the simple model of Fig. 1a and therefore to accurately model the process, another circuit is used which is given in Fig. 1b [37].

## 3.2 Adsorption Isotherm

In order to understand the interaction between carbon steel surface and the inhibitors, the adsorption isotherms are used. The adsorption process depends on several parameters such as the nature and charge of the corroding metal surface, the inhibitor's chemical structure, and the charge distribution in the inhibitor molecules. In the present work, several adsorption isotherms were tested and the best fit was provided by the Langmuir isotherm where a straight line was obtained from the

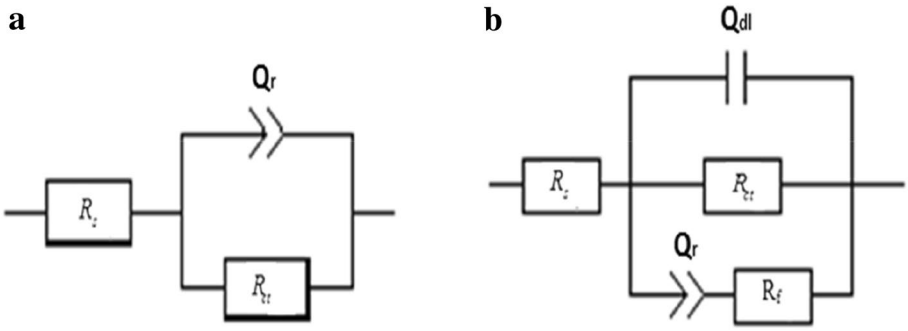


**Fig. 6** Equivalent electrical circuit model used to fit impedance spectra of DPI (**a**) and TPI (**b**)

**Table 1** Impedance parameters of carbon steel in 1.0 M HCl containing different concentrations of the studied compounds

| Medium | Concentration (M) | $R_s$ (Ω cm$^2$) | $R_{ct}$ (Ω cm$^2$) | $R_f$ (Ω cm$^2$) | $Q_r$ (μF s$^{n-1}$) | $Q_{dl}$ (μF) | $n$ | $C_{dl}$ (μF cm$^{-2}$) | IE% |
|---|---|---|---|---|---|---|---|---|---|
| 1.0 M HCl | 00 | 1.123 | 34.7 | *** | 419 | | 0.773 | 121 | – |
| DPI | $10^{-6}$ | 1.506 | 143 | *** | 153 | – | 0.716 | 33.76 | 75.7 |
| | $10^{-5}$ | 1.104 | 147 | *** | 150 | – | 0.610 | 52.83 | 76.4 |
| | $10^{-4}$ | 1.412 | 258 | *** | 172 | – | 0.539 | 12.09 | 86.5 |
| | $10^{-3}$ | 2.259 | 261 | *** | 148 | – | 0.709 | 39.19 | 86.7 |
| TPI | $10^{-6}$ | 3.382 | 198 | 52.88 | 233 | 2.011 | 0.630 | 38.25 | 82.4 |
| | $10^{-5}$ | 1.998 | 225 | 22.35 | 251 | 3.361 | 0.643 | 50.89 | 84.5 |
| | $10^{-4}$ | 4.722 | 302 | 47.73 | 161 | 3.642 | 0.656 | 32.97 | 88.5 |
| | $10^{-3}$ | 3.155 | 306 | 39.00 | 199 | 2.989 | 0.689 | 56.26 | 88.6 |

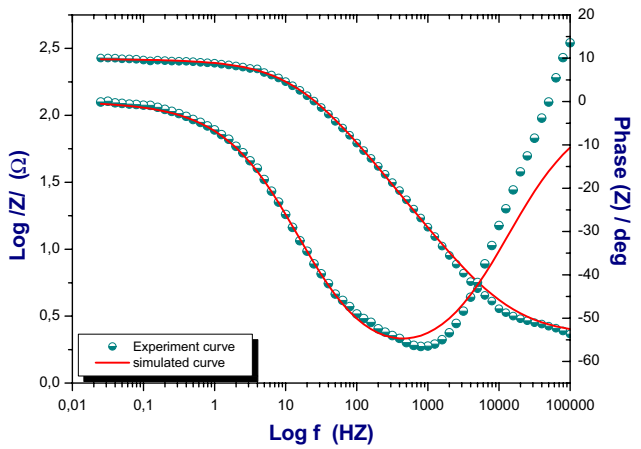


**Fig. 7** Bode diagrams for carbon steel/1.0 M HCl + $10^{-3}$ M of DPI

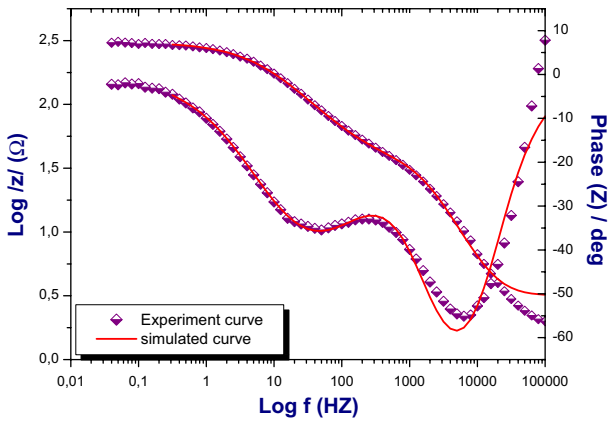


**Fig. 8** Bode diagrams for carbon steel/1.0 M HCl + $10^{-3}$ M of TPI

plot of $C_{inh}/\theta$ versus $C_{inh}$ with a slope around unity (Fig. 9). The Langmuir isotherm can be expressed as

$$\frac{C_{inh}}{\theta} = \frac{1}{K} + C_{inh},$$

$$K_{ads} = \frac{1}{55.5}\exp\left(-\frac{\Delta G^0_{ads}}{RT}\right),$$

where $K_{ads}$ is the adsorption–desorption equilibrium constant and $\Delta G^0_{ads}$ is the standard free energy of adsorption, 55.5 is the value of the molar concentration of water in the solution [39].

From literature, the adsorption of an inhibitor is described as chemisorption if the $\Delta G^0_{ads}$ values are in order of (−40 kJ mol$^{-1}$) or higher and physisorption if $\Delta G^0_{ads}$ values at around −20 kJ mol$^{-1}$ [40, 41] or lower. As can be observed from Table 2, the calculated $\Delta G^0_{ads}$ value around

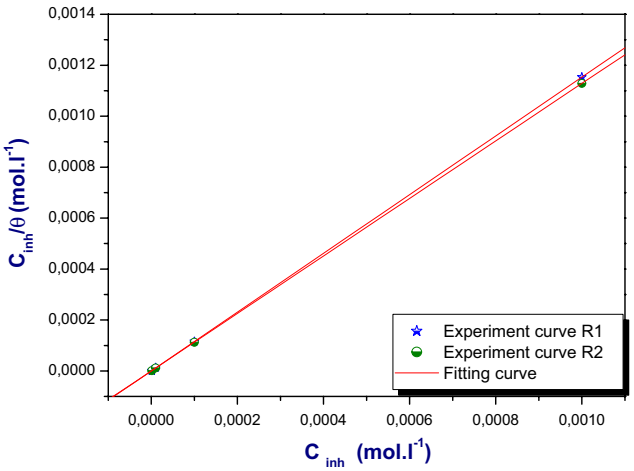


**Fig. 9** Langmuir adsorption isotherm of DPI (R1) and TPI (R2) in 1.0 M HCl at 303 K

**Table 2** Thermodynamic parameters for the adsorption of DPI and TPI in 1.0 M HCl at 303 K

| Inhibitors | Slope | K ($M^{-1}$) | $\Delta G^0_{ads}$ (KJ $mol^{-1}$) |
|---|---|---|---|
| DPI | 1.15 | $1.43\times10^6$ | −45.8 |
| TPI | 1.12 | $3.76\times10^6$ | −48.2 |

−40 kJ $mol^{-1}$ signifies that the adsorption mechanism of both the inhibitors tested on carbon steel surface in 1.0 M HCl solution is distinctively a chemisorption [42–44].

## 3.3 Effect of Temperature

The temperature is one of the parameters which can change the interaction between the carbon steel surface and the acidic solution without and with inhibitor. The Nyquist plots of carbon steel in 1.0 M HCl with and without different concentrations of inhibitors in the temperature range from 303 to 333 K are shown in Fig. 10.

The Nyquist diagrams obtained for DPI at different temperatures obey to the circuit given in Fig. 1a. On the other hand, the Nyquist plots of inhibitor (TPI) at different temperatures follow the second circuit, as it was observed for the study of the effect of concentration. The various electrochemical parameters were calculated and are summarized in Table 3.

It can be observed from Table 3 that the $R_{ct}$ increased with increase in temperature in inhibited solutions. Consequently, the values of inhibition efficiency increased to attain 95.7% at $10^{-3}$ M concentration at 333 K. This may be attributed to the formation of a protective film of TPI on the electrode surface [45–47].

On the other hand, the values of surface coverage θ for different inhibitor concentrations were tested by fitting to various isotherms but the finest one obtained is Langmuir isotherm because it had a slope around unity. The parameters of adsorption are shown in Table 4.

The values of $\Delta G^0_{ads}$ for the studied inhibitors is greater than −40 kJ/mol which indicates that TPI molecules may get adsorbed with a chemisorption interaction type as reported in literature. In other words, this inhibitor may get adsorbed onto the metal surface by making strong bonds [48–50] (Fig. 11).

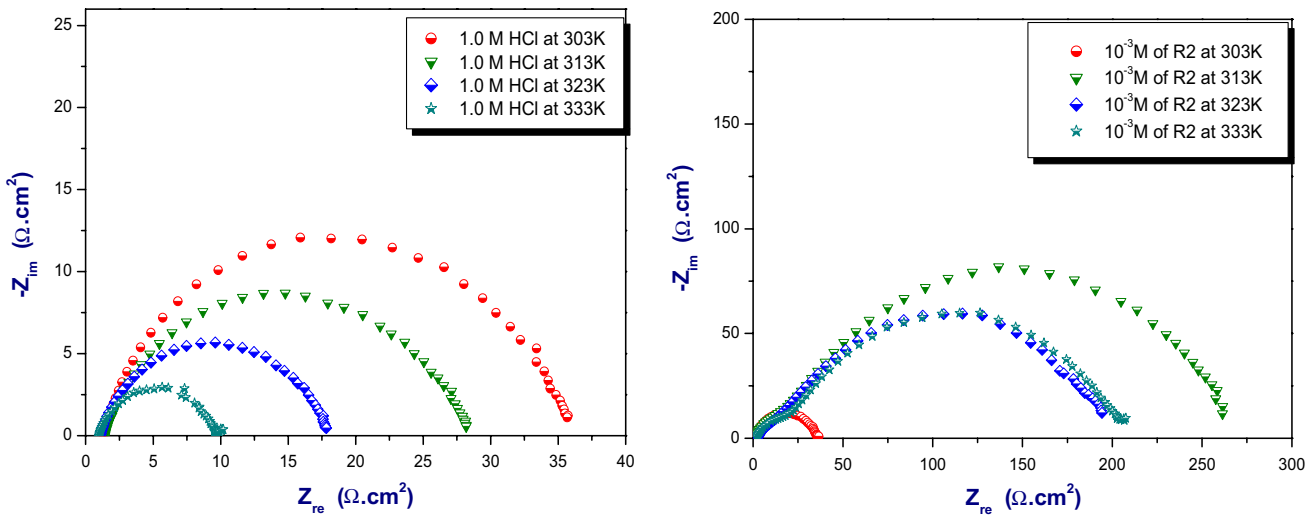


**Fig. 10** Nyquist plots for carbon steel in 1.0 M HCl without and with optimal concentration of TPI (R2) at different temperatures

**Table 3** Impedance parameters of carbon steel in 1.0 M HCl at different temperatures without and with different concentrations of TPI

| System | T (K) | C (M) | $R_{ct}$ (Ω cm$^2$) | $C_{dl}$ (μF cm$^{-2}$) | IE% |
|---|---|---|---|---|---|
| HCl | 313 | 1 | 27.1 | 75.65 | – |
| | 323 | 1 | 17.0 | 74.1 | – |
| | 333 | 1 | 8.7 | 99.45 | – |
| TPI | 313 | $10^{-6}$ | 37.6 | 84.63 | 27.9 |
| | | $10^{-5}$ | 63.6 | 22.9 | 57.3 |
| | | $10^{-4}$ | 210.0 | 1.53 | 87.1 |
| | | $10^{-3}$ | 268.3 | 2.22 | 89.0 |
| | 323 | $10^{-6}$ | 28.3 | 30.63 | 39.9 |
| | | $10^{-5}$ | 48.0 | 33.5 | 64.5 |
| | | $10^{-4}$ | 87.6 | 8.17 | 80.5 |
| | | $10^{-3}$ | 196.0 | 1.99 | 91.3 |
| | 333 | $10^{-6}$ | 21.4 | 24.68 | 59.3 |
| | | $10^{-5}$ | 26.7 | 23.37 | 67.4 |
| | | $10^{-4}$ | 134.0 | 3.72 | 93.5 |
| | | $10^{-3}$ | 204.6 | 1.29 | 95.7 |

**Table 4** Thermodynamic parameters for the adsorption of TPI in 1.0 M HCl at different temperatures

| Inhibitor | Temperature (K) | Slope | K ($M^{-1}$) | $\Delta G^0_{ads}$ (kJ mol$^{-1}$) |
|---|---|---|---|---|
| TPI | 313 | 1.11 | $2.58\times10^5$ | −41.5 |
| | 323 | 1.08 | $1.46\times0^5$ | −40.1 |
| | 333 | 1.04 | $3.88\times10^5$ | −42.5 |

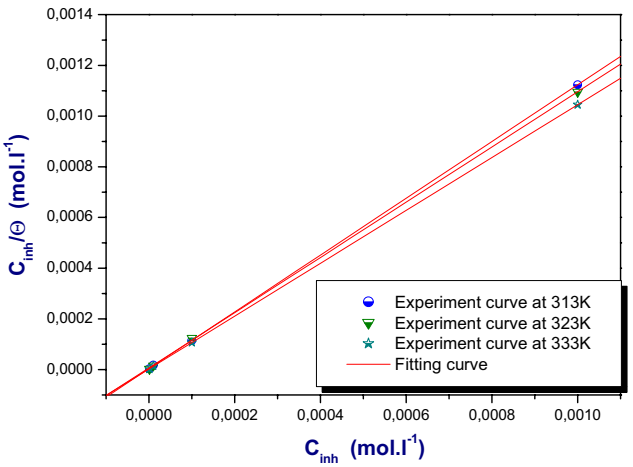


**Fig. 11** Langmuir adsorption isotherm of TPI in 1.0 M HCl at different temperatures

## 3.4 Effect of Immersion Time

The electrochemical impedance spectroscopy is a useful technique for testing the corrosion inhibition process at long immersion time. These experiments were carried out

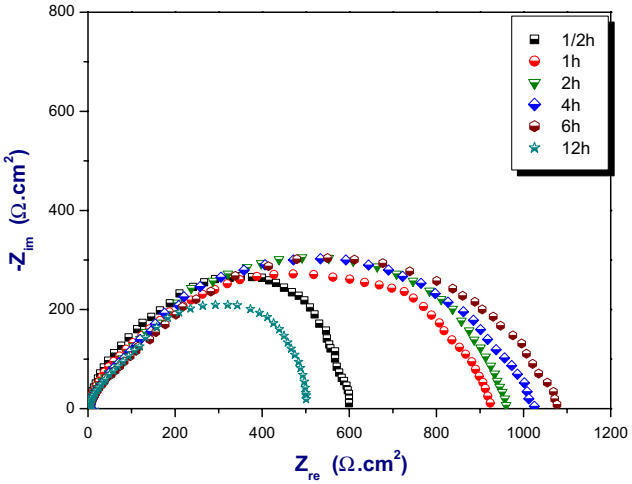


**Fig. 12** Impedance spectra obtained after different immersion times in 1.0 M HCl solution with optimal concentration of TPI

**Table 5** Electrochemical impedance parameters for C-steel in 1.0 M HCl solution with and without optimum concentration of inhibitor at different immersion times

| Medium | Time (h) | $R_s$ (Ω cm$^2$) | $R_{ct}$ (Ω cm$^2$) | $C_{dl}$ (μF/cm$^2$) | IE% |
|---|---|---|---|---|---|
| 1.0 M HCl | ½ | 0.5 | 37.7 | 105 | – |
| | 1 | 1.2 | 28 | 142 | – |
| | 2 | 1.01 | 23 | 226 | – |
| | 4 | 1.02 | 20 | 291 | – |
| | 6 | 0.99 | 19.5 | 302 | – |
| | 12 | 1.3 | 11.7 | 345 | – |
| TPI | ½ | 3.1 | 598 | 20.5 | 93.6 |
| | 1 | 3.4 | 923 | 18.8 | 96.9 |
| | 2 | 4.2 | 958 | 18.2 | 97.5 |
| | 4 | 9.2 | 1025 | 16.1 | 98.0 |
| | 6 | 5.2 | 1077 | 9.3 | 98.1 |
| | 12 | 5.4 | 1030 | 14.9 | 97.6 |

in order to follow the evolution of phenomena occurring at the metal–solution interface at different immersion times from 1/2 to 12 h. Figure 12 shows the evolution of the impedance spectra at different immersion times in 1.0 M HCl solution containing optimal concentrations of the tested inhibitor TPI.

The electrochemical impedance parameters given in Table 5 show the variation of the $R_{ct}$ as a function of the immersion time. The $R_{ct}$ increases with increase in immersion time to achieve a value of 1077 Ω cm$^2$ after 6 h and then decreases slightly afterwards to attain 1030 Ω cm$^2$ after 12 h of immersion time. This behavior indicates that the protective film formed was getting strong until 6 h. In other words, the protective properties of the film formed on the surface of C-steel are reinforced until 6 h

of immersion time. Further, this film is liable to dissolve at higher immersion time [51–53].

### 3.5 DFT Study

The experimental results provide evidence of the inhibition efficiency of the molecules tested in this study, which may act through a chemical adsorption mechanism. From the experimental results, it was observed that the TPI showed a higher corrosion inhibition efficiency compared to DPI. Therefore, to obtain a thorough understanding of the electronic interaction between the inhibitor molecules and the metallic surface, several theoretical parameters such as the molecular orbital energies ($E_{HOMO}$, $E_{LUMO}$) were determined and are listed in Table 6.

The frontier molecular orbital surfaces provide information about the highest occupied molecular orbital (HOMO) of the inhibitor that may be responsible for donation of electrons to the vacant d-orbital of the metal and the lowest unoccupied molecular orbital (LUMO) of the inhibitor that may be liable to accept a pair of electrons from an electron-rich metal surface during back-bonding. Thus, smaller values of the ΔE correspond to higher inhibition efficiencies of the compound [54–57] which explains the high stability of the compound in the complex formed with the mild steel surface. The HOMO and LUMO density distributions of the optimized structures are shown in Fig. 13. It can be observed that the HOMO of DPI and TPI are essentially localized on the carbon chain. In contrast, The LUMO surfaces of these inhibitors are mostly distributed on the Pyridazinium ring. This may be due to the presence of highly electronegative nitrogen atoms in the Pyridazinium ring, which can make the ring to be relatively electron-deficient and the fact that it is a cationic moiety. Therefore, only the cations interact with the metal surface by the pyridazine ring which can be explained by the transfer of the electron from d-orbital of Fe to vacant orbital of pyridazine ring in purpose to form feedback coordinate bond [57]; this can be further confirmed by the negative value of ΔN as shown in Table 6.

**Table 6** Quantum chemical parameters of the studied inhibitors

| Inhibitors | Quantum chemical parameters | | | | | | | |
|---|---|---|---|---|---|---|---|---|
| | Dipole moment (Debye) | $E_{HOMO}$ (eV) | $E_{LUMO}$ (eV) | ΔE (eV) | Hardness ($\eta$) | Softness ($\sigma$) | Electronegativity ($\chi$) | ΔN |
| DPI | 21.027 | −9.899 | −7.088 | 2.811 | 1.405 | 0.711 | 8.494 | −0.531 |
| TPI | 32.552 | −9.187 | −7.084 | 2.102 | 1.051 | 0.951 | 8.135 | −0.540 |

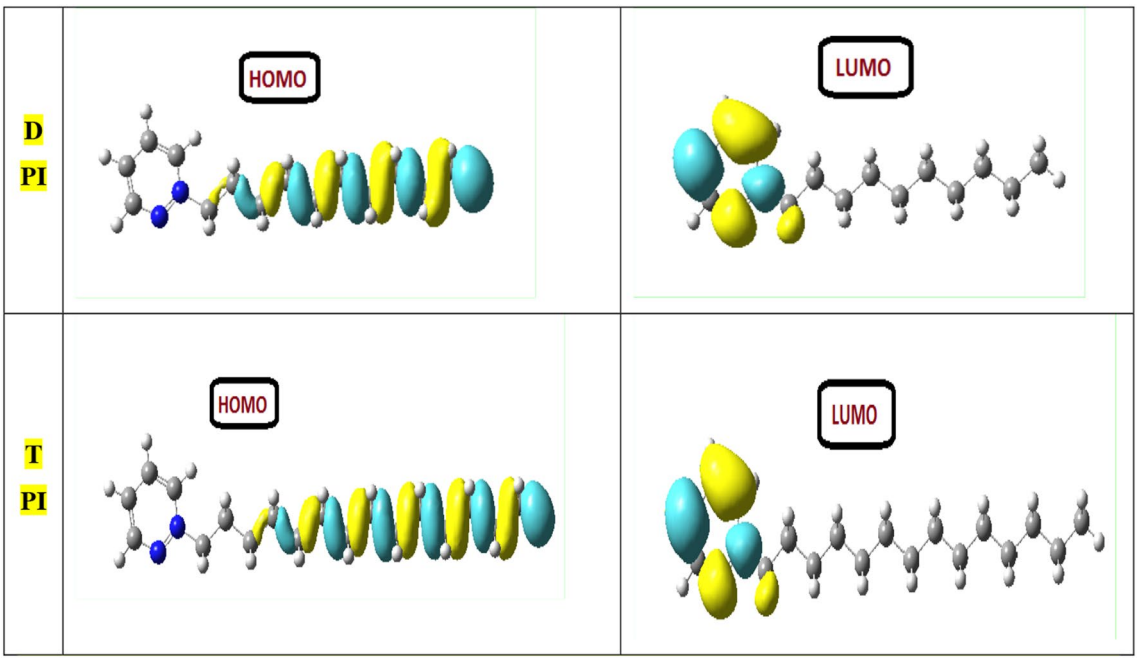


**Fig. 13** Frontier molecule orbitals density distributions of DPI and TPI at B3LYP/6-31G (d, p) level of theory

The data provided in Table 6 show that TPI has a higher value of $E_{HOMO}$ which shows a higher tendency to donate electrons to the metal surface and could be the reason behind the higher obtained inhibition efficiency of TPI compared to DPI. Moreover, the results in Table 6 show that TPI has a lower energy gap ($\Delta E$) than DPI. This means higher reactivity with mild steel, which is again in agreement with its higher inhibition efficiency obtained experimentally. Further, a lower value of global hardness and consequently a higher value of global softness suggest better reactivity of TPI compared to DPI. The fraction of electrons transferred ($\Delta$N) describes the inhibition achieved from electron donation. If $\Delta N < 3.6$, the inhibition efficiency increases with increasing electron-donation ability to the metal surface [58–60] which explains the higher reactivity of inhibitor TPI than DPI. Also, as shown in Table 6, the $\mu$ for ATP cation is higher than that for DPI which owing to the dipole–dipole interaction between inhibitor molecules and metal surface, the higher value of μ in case of TPI may lead to stronger inhibition.

## 4 Conclusions

The inhibition effects of pyridazine derivatives against corrosion of carbon steel were tested using different concentrations and at various temperatures in 1.0 M HCl by electrochemical impedance spectroscopy (EIS). Both ionic liquids inhibit corrosion with inhibition efficiency higher than 86% at $10^{-3}$ M and which increased to 95.7% at $10^{-3}$ M at 333 K for TPI. The charge transfer resistance showed an increase with a decrease in the double-layer capacitance which indicated the adsorption of the inhibitors on the metal/ solution interface. The adsorption became more remarkable with increase in temperature as observed by EIS data. The adsorption of inhibitors tested on to the steel surface in the studied acidic solution obeyed the Langmuir isotherm and the values of $\Delta G^0_{ads}$ indicate that both the inhibitors undergo chemical adsorption over the metal surface leading to the formation of a strong protective film. This adsorption is more pronounced at longer immersion time because this inhibitor achieves good inhibition efficiency although after an immersion period of 12 h. Quantum chemical calculations were used to provide a molecular level understanding of the mechanism of the interaction of the inhibitor molecules with steel surface and the computational data showed a good agreement with the experimentally obtained results.

## References


1. Rani BESA, Basu BBJ (2012) Green inhibitors for corrosion protection of metals and alloys: an overview. Int J Corros 2012:15
2. Zarrok H, Oudda H, El Midaoui A, Zarrouk A, Hammouti B, Touhami ME, Attayibat A, Radi S, Touzani R (2012) Some new bipyrazole derivatives as corrosion inhibitors for C38 steel in acidic medium. Res Chem Intermed 38:2051
3. Hmamou DB, Salghi R, Zarrouk A, Zarrok H, Hammouti B, Al-Deyab SS, ElAssyry A, Benchat N, Bouachrine M (2013) Electrochemical and gravimetric evaluation of 7-methyl-2-phenylimidazo[1,2-á]pyridine of carbon steel corrosion in phosphoric acid solution. Int J Electrochem Sci 8:11526
4. Shahabi S, Norouzi P, Ganjali MR (2015) Theoretical and electrochemical study of carbon steel corrosion inhibition in the presence of two synthesized schiff base inhibitors: application of fast fourier transform continuous cyclic voltammetry to study the adsorption behavior. Int J Electrochem Sci 10:2646
5. Banua VRN, Rajendran S, Kumaran SS (2016) Investigation of the inhibitive effect of Tween 20 self-assembling nanofilms on corrosion of carbon steel. J Alloy Compd 675:139
6. Bouzidi D, Kertit S, Hammouti B, Brighli M (1997) Someaminoacids and aminoesters as non-toxic inhibitors for the corrosion of iron in 0.5 M $H_2SO_4$. J Electrochem Soc India 46:23
7. Ghazoui A, Zarrouk A, Benchat N, Salghi R, Assouag M, El Hezzat M, Guenbour A, Hammouti B (2014) New possibility of mild steel corrosion inhibition by organic heterocyclic compound. J Chem Pharm Res 6:704
8. Swathi NP, Alva VDP, Samshuddin S (2017) A Review on 1,2,4-triazole derivatives as corrosion inhibitors. J Bio Tribo Corros 3:42
9. Zarrouk A, Hammouti B, Zarrok H, Bouachrine M, Khaled KF, Al-Deyab SS (2012) Corrosion inhibition of copper in nitric acid solutions using a new triazole derivative. Int J Electrochem Sci 7:89
10. Nahle A, El-Hajjaji F, Ghazoui A, Benchat NE, Taleb M, Saddik R, Elaatiaoui A, Koudad M, Hammouti B (2018) Effect of substituted methyl group by phenyl group in pyridazine ring on the corrosion inhibition of mild steel in 1.0 M HCl. Anti-Corros Methods Mater 65:87
11. Bouoidina A, Chaouch M, Abdellaoui A, Lahkimi A, Hammouti B, El-Hajjaji F, Taleb M, NahleA (2017) Essential oil of "Foeniculumvulgare": antioxidant and corrosion inhibitor on mild steel immersed in hydrochloric medium. Anti-Corros Methods Mater 64:563
12. Mousavi M, Mohammadalizadeh M, Khosravan A (2011)Theoretical investigation of corrosion inhibition effect of imidazole and its derivatives on mild steel using cluster model. Corros Sci 53:3086
13. Abdallah M, Megahed HE, Sobhi M (2010) $Ni^{2+}$ cation and imidazole as corrosion inhibitors for carbon steel in sulfuric acid solutions. Monatsh Chem 141:1287
14. Benabdellah M, Yahyi A, Dafali A, Aouniti A, Hammouti B, Ettouhami A (2011) Corrosion inhibition of steel in molar HCl by triphenyltin2–thiophene carboxylate. Arab J Chem 4:243
15. ElBakri Y, Boudalia M, Echihi S, Harmaoui A, Sebhaoui J, Elmsellem H, Ali AB, Ramli Y, Guenbour A, Bellaouchou A, Essassi EM (2017) Performance and theoretical study on corrosion inhibition of new triazolopyrimidine derivative for carbon steel in hydrochloric acid. J Mater Environ Sci 8:378
16. Agi A, Junin R, Zakariah MI (2018) Effect of temperature and acid concentration on rhizophoramucronata tannin as a corrosion inhibitor. J Bio Tribo Corros 4:5
17. Yadav M, Behera D, Kumar S (2014) Experimental and theoretical investigation on adsorption and corrosion inhibition properties of imidazopyridine derivatives on mild steel in hydrochloric acid solution. Surf Interface Anal 46:640
18. Verma C, Ebenso EE, Quraishi MA (2017) Ionic liquids as green and sustainable corrosion inhibitors for metals and alloys: an overview. J Mol Liq 233:403

19. Liu JF, Jiang GB, Chi YG, Cai YQ, Zhou QX, Hu JT (2003) Use of ionic liquids for liquid-phase microextraction of polycyclic aromatic hydrocarbons. Anal Chem 75:5870
20. Ibrahim MA, Messali M (2011) Ionic liquid [BMPy]Br as an effective additives during Zinc electrodeposition from aqueous sulphate bath. Prod Finish 2:14
21. Ue M, Takeda M, Toriumi A, Kominato A, Hagiwara R, Ito Y (2003) Application of low-viscosity ionic liquid to the electrolyte of double-layer capacitors. J Electrochem Soc 150:499
22. Brennecke JF, Maginn E (2001) Ionic liquids: innovative fluids for chemical processing. AIChE J 47:2384
23. Messali M (2011) A green microwave-assisted synthesis, characterization and comparative study of new pyridazinium-based ionic liquids derivatives towards corrosion of mild steel in in acidic environment. J Mater Environ Sci 2:174
24. El-Hajjaji F, Messali M, Aljuhani A, Aouad MR, Hammouti B, Belghiti ME, Chauhan DS, Quraishi MA (2018) Pyridazinium-based ionic liquids as novel and green corrosion inhibitors of carbon steel in acid medium: electrochemical and molecular dynamics simulation studies. J Mol Liq 249:997
25. Zarrouk A, Messali M, Zarrok H, Salghi R, Ali A, Hammouti B, Al-Deyab S, Bentiss F(2012) Synthesis, characterization and comparative study of new functionalized imidazolium-based ionic liquids derivatives towards corrosion of C38 steel in molar hydrochloric acid. Int J Electrochem Sci 7:6998
26. Lopez DA, Simison SN, de Sanchez SR(2003) The influence of steel microstructure on $CO_2$ corrosion: EIS studies on the inhibition efficiency of benzimidazole. Electrochim Acta 48:845
27. Pearson RG (1988) Absolute electronegativity and hardness: application to inorganic chemistry. Inorg Chem 27:734
28. Zarrouk A, Messali M, Aouad M, Zarrok H, Salghi R, Hammouti B, Chetouani A, Al-Deyab S (2012) Some new ionic liquids derivatives: synthesis, characterization and comparative study towards corrosion of C-steel in acidic media. J Chem Pharm Res 4:3427
29. Al-Ghamdi AF, Messali M, Ahmed SA (2011) Electrochemical studies of new pyridazinium-based ionic liquid and its determination in different detergents. J Mater Environ Sci 2:215
30. Messali M (2014) An efficient and green sonochemical synthesis of some new eco-friendly functionalized ionic liquids. Arab J Chem 7:63
31. Ghazoui A, Benchat N, El-Hajjaji F, Taleb M, Rais Z, Saddik R, Elaatiaoui A, Hammouti B (2017) The study of the effect of ethyl (6-methyl-3-oxopyridazin-2-yl) acetate on mild steel corrosion in 1 M HCl. J Alloys Compd 693:510
32. Solmaz R (2014) Investigation of adsorption and corrosion inhibition of mild steel in hydrochloric acid solution by 5-(4-dimethylaminobenzylydene. Rhodanine Corros Sci 79:169
33. Bousskri A, Anejjar A, Messali M, Salghi R, Benali O, Karzazi Y, Jodeh S, Zougagh M, Ebenso EE, Hammouti B (2015) Corrosion inhibition of carbon steel in aggressive acidic media with 1-(2-(4-chlorophenyl)-2-oxoethyl)pyridazinium bromide. J Mol Liq 211:1000
34. El-Hajjaji F, Belghiti ME, Hammouti B, Jodeh S, Hamec O, Lgaz H, Salghi R(2018) Adsorption and corrosion inhibition effect of 2-mercaptobenzimidazole (surfactant) on a carbon steel surface in an acidic medium: experimental and monte carlo simulations. Portugaliae Electrochim Acta 36:197
35. Bousskri A, Anejjar A, Salghi R, Jodeh S, Touzani R, Bazzi L, Lgaz H (2016) Corrosion control of carbon steel in hydrochloric acid by new eco-friendly picolinium-based ionic liquids derivative: electrochemical and synergistic studies. J Mater Environ Sci 7:4269
36. Si˘gircik G, T¨uken T, Erbil M (2016) Assessment of the inhibition efficiency of 3,4-diaminobenzonitrile against the corrosion of steel. Corros Sci 102:437
37. Popova A, Christov M (2006) Evaluation of impedance measurements on mild steel corrosion in acid media in the presence of heterocyclic compounds. Corros Sci 48:3208
38. Yadav DK, Chauhan DS, Ahamad I, Quraishi MA (2013) Electrochemical behavior of steel/acid interface: adsorption and inhibition effect of oligomeric aniline. RSC Adv 3:632
39. Jafari H, Sayin K, Mohsenifar F (2017) Measuring adsorption behavior and corrosion inhibition of trans and cis of di-(3-hydroxybenzaldehyde)-1,2-diaminocyclohexane. J Bio Tribo Corros 3:48
40. Finley HF, Hackerman N (1960) Effect of adsorption of polar organic compounds on the reactivity of steel. J Electrochem Soc 107:259
41. Hayaoui M, Drissi M, Fahim M, Salim R, Rais Z, Mouffarih S, Baba MF, El Hajjaji F, Zarrouk A, Taleb M (2017) Benzenamine derivative as corrosion inhibitor of carbon steel in hydrochloric acid solution: Electrochemical and theoretical studies. J Mater Environ Sci 8:1877
42. ElOuasif L, Merimi I, Zarrok H, Elghoul M, Achour R, Guenbour M, Oudda H, El-Hajjaji F, Hammouti B (2016) Synthesis and inhibition study of carbon steel corrosion in hydrochloric acid of a new surfactant derived from 2-mercaptobenzimidazole. J Mater Environ Sci 7:2718
43. Ghazoui A, Benchat N, El-Hajjaji F, Taleb M, Rais Z, Saddik R, Elaatiaoui A, Hammouti B (2017) The study of the effect of ethyl (6-methyl-3-oxopyridazin-2-yl) acetate on mild steel corrosion in 1 M HCl. J Alloy Compd 693:510
44. Verma CB, Quraishi MA, Ebenso EE (2014) Application of some oligopolymers as effective corrosion inhibitors for mild steel in 1 M HCl: gravimetric, thermodynamic and electrochemical analysis. Int J Electrochem Sci 9:5507
45. Gupta NK, Haque J, Salghi R (2018) Spiro [indoline-3,4′-pyrano[2,3-c]pyrazole] derivatives as novel class of green corrosion inhibitors for mild steel in hydrochloric acid medium: theoretical and experimental approach. J Bio Tribo Corros 4:16
46. Verma C, Reddy MJ, Quraishi MA (2014) Microwave assisted eco-friendly synthesis of chalcones using 2, 4-dihydroxy acetophenone and aldehydes as corrosion inhibitors for mild steel in 1 M HCl. Anal Bioanal Electrochem 6:321
47. Ahamad I, Prasad R, Quraishi MA (2010) Adsorption and inhibitive properties of some new Mannich bases of Isatin derivatives on corrosion of mild steel in acidic media. Corros Sci 52:1472
48. Abd El-Lateef HM (2015) Experimental and computational investigation on the corrosion inhibition characteristics of mild steel by some novel synthesized imines in hydrochloric acid solutions. Corros Sci 92:104
49. Hamani H, Douadi T, Daoud D, Al-Noaimi M, Rikkouh RA, Chafaa S (2017) 1-(4-Nitrophenylo-imino)-1-(phenylhydrazono)-propan-2-one as corrosion inhibitor for mild steel in 1 M HCl solution: weight loss, electrochemical, thermodynamic and quantum chemical studies. J Electroanal Chem 801:425
50. Salim R, Elaatiaoui A, Benchat N, Ech-Chihbi E, Rais Z, Oudda H, El Hajjaji F, ElAoufir Y, Taleb M (2017) Corrosion behavior of a smart inhibitor in hydrochloric acid molar: experimental and theoretical studies. J Mater Environ Sci 8:3747
51. Verma C, Quraishi MA, Ebenso EE (2018) A green and sustainable approach for mild steel acidic corrosion inhibition using leaves extract: experimental and DFT studies. J Bio Tribo Corros 4:33
52. Elhousni L, Galai M, El Kamraoui FZ, Dkhireche N, Touhami ME, Touir R, Chebabe D, Sfaira M, Zarrouk A (2016) Study of sodium gluconate and cetyltrimethyl ammonium bromide as inhibitor for copper in Moroccan industrial cooling water systems. J Mater Environ Sci 7:2513
53. Ech-Chihbi E, Belghiti ME, Salim R, Oudda H, Taleb M, Benchat N, Hammouti B, El-Hajjaji F (2017) Experimental and computational studies on the inhibition performance of the organic

compound "2-phenylimidazo [1,2-a]pyrimidine-3-carbaldehyde" against the corrosion of carbon steel in 1.0 M HCl solution. Surf Interfaces 9:206
54. Motsie EM, Lukman OO, Abolanle SA, Sasikumar Y, Mwadham MK, Eno EE (2015) Adsorption, thermodynamic and quantum chemical studies of 1-hexyl-3-methylimidazolium based ionic liquids as corrosion inhibitors for mild steel in HCl. Materials 8:3607
55. Sasikumar Y, Adekunle AS, Olasunkanmi LO, Bahadur I, Baskar R, Kabanda MM, Obot IB, Ebenso EE (2015) Experimental, quantum chemical and Monte Carlo simulation studies on the corrosion inhibition of some alkyl imidazolium ionic liquids containing tetrafluoroborate anion on mild steel in acidic medium. J Mol Liq 211:105
56. Chauhan DS, Ansari KR, Sorour AA, Quraishi MA, Lgaz H, Salghi R (2018) Thiosemicarbazide and thiocarbohydrazide functionalized chitosan as ecofriendly corrosion inhibitors for carbon steel in hydrochloric acid solution. Int J Biol Macromol 107:1747
57. Srivastava V, Chauhan DS, Joshi PG (2018) PEG-functionalized chitosan: a biological macromolecule as a novel corrosion inhibitor. Chem Select 3:1990
58. Zheng X, Zhang S, Li W, Gong M, Yin L (2015) Experimental and theoretical studies of two imidazolium-based ionic liquids as inhibitors for mild steel in sulfuric acid solution. Corros Sci 95:168
59. Haque J, Srivastava V, Chauhan DS, Lgaz H, Quraishi MA (2018) Microwave-induced synthesis of chitosan Schiff bases and their application as novel and green corrosion inhibitors: experimental and theoretical approach. ACS Omega 3:5654
60. Dohare P, Chauhan DS, Sorour AA, Quraishi MA (2017) DFT and experimental studies on the inhibition potentials of expired Tramadol drug on mild steel corrosion in hydrochloric acid. Mater Discov 9:30